THE ELECTRO-OPTIC SAMPLING STATIONS FOR FERMI@Elettra, A DESIGN STUDY

M. Veronese*, M. Danailov, M. Ferianis, Sincrotrone Trieste, Trieste, Italy

Abstract

FERMI@Elettra is a seeded FEL source, currently under construction at the Elettra Synchrotron Light Laboratory. On-line single shot and non destructive longitudinal bunch profile and bunch arrival time measurements are of great importance for this type of FEL source. These measurements will be performed by means of two Electro Optic Station (EOS) to be installed just upstream each of the two undulator chains. The paper describes the EOS stations design based on the spatial conversion scheme tested at SPPS and FLASH, and proposed for LCLS. The EOS will make use of two laser sources: a fiber laser at 780nm and the seed laser oscillator. A set of ZnTe and GaP crystal of different thicknesses will allow for flexibility in choosing high signal or high resolution configurations. The maximum resolution is expected to be of about100 fsec. The time profile mapped in a spatial laser profile will be acquired by a gated Intensified CCD.Calculations are presented for the expected EO signal and THz pulse broadening and distortion during propagation in the crystals.

MACHINE PARAMETERS

FERMI@Elettra is an single pass seeded FEL under construction at the Sincrotrone Trieste Laboratory, based on a normal conducting Linac (50Hz repetition rate), designed to laser in the range from 100nm to 10nm. A general description of the machine is presented in the FERMI Conceptual Design Report [1]. Two main operation configurations of the machine are foreseen: the *Medium Bunch* and the *Short Bunch*. The main machine parameters at EOS location are summarized in table 1. Two identical EOS stations are foreseen one per each of the two (FEL1 and FEL2) undulator chains. The aim is to provide a high resolution single shot non destructive longitudinal profile and bunch arrival time measurement with very low time jitter. The the SPPS-DESY spatial decoding scheme [2], [3] has beem adopted since it does not require an amplifier laser system and temporal resolution of about 150fsec has been demonstrated.

Table 1: FERMI@Elettra EOS main machine parameters.

Parameter	Medium Bunch	Short Bunch
Energy	1.2 GeV	1.2 GeV
Bunch Length FW	0.9 ps	0.17 ps
Charge	1 nC	0.5 nC
Beta (β_x, β_y)	(14m,7m)	(14m,7m)
Alpha (α_x, α_y)	(0.5,-0.5)	(0.5,-0.5)
Beam Size X (σ_x)	110 μm	110μm
Beam Size Y (σ_y)	77 μm	77 μm

LASER SOURCES

Femtosecond laser pulses from two different sources are foreseen for the spatial decoding scheme. The initial operation will be performed using a Menlosystems TC-780 fiber laser to be installed in the tunnel. The laser provides pulses at repetition rate of 78.895 MHz, with 120 fsec pulse width, and 0.8 nJ of energy per pulse. It offers noticeable performances in terms of temporal jitter with only 20fsec RMS (10Hz-1MHz) time jitter with respect to its electrical reference. This laser will allow operation from the very first days of the commissioning of FERMI in a very reliable way and is a *turn key* system.

When the ultrastable timing and synchronization distribution system will be installed we plan to use pulses from the fiber timing and synchronization distribution system (based on the MIT-DESY design). The pulses amplified by an EDFA amplifier and are used for second harmonic generation, bringing the wavelength down to 780nm. In this way we will intrinsically synchronized the ultra stable reference that will also be distributed to the users. The expected bunch arrival time jitter will then be only limited by the relative jitter between fiber links which we expect to be less than 10fsec RMS.

SETUP

The EOS stations will be located just upstream of the modulator, the first module of the FEL undulators chain. An optical table will support both fiber laser sources, all optical components and the vacuum chamber housing the EO crystals as well as the detector. For the whole length of the optical table the vacuum chamber will be supported on the table while at both ends bellows will isolate the EOS from the rest of the machine to guarantee maximum vibration isolation. A cavity BPM will be in the immediate vicinity and will allow for position measurements with micron accuracy. The whole setup including the vacuum chamber will be isolated from the rest of the tunnel by a light tight enclosure to prevent ambient light, air turbulence and for laser related safety issues too.

The EOS layout is sketched in figure 1. The laser source selection will be provided by a remotely movable mirror. A prism compressor is foreseen to reduce the temporal duration of the pulses to below 100 fsec. A remotely controlled

* marco.veronese@elettra.trieste.it

$\lambda/2$ and a polarizer will allow for adjustment of the laser power. A beam splitter will spill a small portion of the energy for laser diagnostics: on line measurements of power stability with a diode and pulse width measurements with a scanning autocorrelator. The main beam will be then directed to a motorized optical delay line to provide timing adjustment. A $\lambda/2$ wave plate will allow for polarization orientation control. Before entering the vacuum chamber the laser beam will pass trough a cylindrical lens to probe the electric field due to the e-beam only at specific distance avoiding averaging over distance. The laser beam will then be steered to the EO crystal with an angle of about 30 degrees with respect to the normal to the EO crystal (the normal is parallel to the electron beam direction). The angle is chosen to optimized for EO signal broadening effect due to group velocity mismatch between laser pulse and THz pulse propagation. Micrometric positioning in both transverse and vertical directions of the in vacuum crystal holder is needed. Multiple crystal (zinc-blende structure cut along (110) plane) are foreseen: 1mm thick ZnTe crystal will provide the highest EO signal and will be used for initial setup of the system, while maximum resolution will be achieved by a 60 μm thick GaP crystal, finally an 0.2mm thick ZnTe will be installed as a backup.

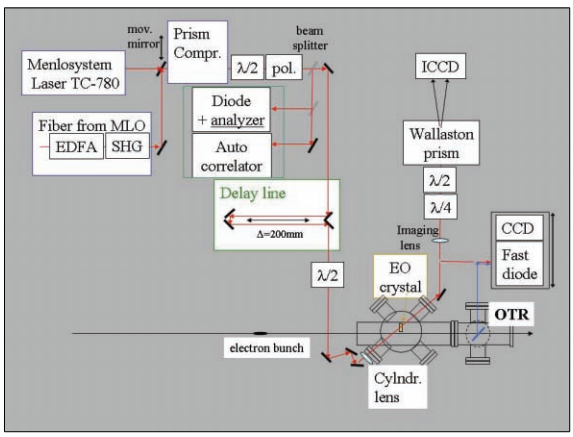

Figure 1: Electro Optical Sampling station layout.

After passing the EO crystal the laser pulse reaches the first lens which will image the EO surface on to the detector. Polarization analysis to extract the phase retardation information will be performed by a $\lambda/4$ zero order wave plate followed by a $\lambda/2$ zero order wave plate both mounted on motorized rotators that can be remotely controlled. Finally a polarizing cube or a Wollaston prism will be used to separate the two polarization components. The single shot image acquisition will be performed by a gated Intensified CCD. A gating time of 10nsec will be sufficient to extract the information from 78.895MHz fiber laser pulse train. Coarse timing alignment will be performed with a fast photodiode measuring at the same time the optical transition radiation from a metallic screen inserted on the electron beam path and the laser pulse.

EO CALCULATIONS

A numerical evaluation of the EO signal for the FERMI@Elettra case has been performed following [6]. Estimate the strength of the EO effect and the achievable resolution for our machine parameters are given.
For ultra-relativistic electrons the electric field has a large transverse component. For a single electron the electric field on axis at a distance b from the electron propagation direction is:

$$E_{y=b} = \frac{e}{4\pi\epsilon_0}\frac{\gamma b}{(b^2+\gamma^2 z^2)^{3/2}} \quad (1)$$

For an electron bunch with N_e electrons, the normalized longitudinal distribution $\rho(z)$ can be approximated for the FERMI case to a rectangular distribution that is conveniently modeled by the difference of two Heaviside functions: $\rho(z) = H(z + FW \cdot c/2) - H(z - FW \cdot c/2)$.
Then the total field along the axis is then:

$$E_{beam} = \int \rho(z - z')E_{0,b,z'}dz' \quad (2)$$

The seed laser travels collinear to the electron beam focusing from its entrance upstream the EOS to reach it minimum width at the center of the modulator. At the position of EOS the half width of the laser beam is expected to be 1.5mm posing a constraint to the minimum distance e-beam crystal. In practice we should consider for our purposes the minimum distance $b = 5$mm. Then for a rectangular distribution and the electron bunch parameters of table 1 we get: 13 MV/m for the $MediumBunch$ and 35MV/m for the $ShortBunch$.
To evaluate the amplitude of the EO effect we consider the case of a laser pulse probing a a crystal of zinc-blende crystal structure like ZnTe or GaP cut crystal along the normal to the (110) plane and a detection based on the $\lambda/4$ + Wollaston prism + balanced detector setup. Then the EOS signal is proportional to $\sin(\Gamma)$ where γ is the phase retardation induced by the electric field of the electron beam as from eq. 3.

$$\Gamma = \frac{\pi d}{\lambda_0} n_0^3 E_{beam} r_{41} \sqrt{1 + 3\cos^2(\alpha)} \quad (3)$$

Where d is the thickness of the crystal, λ_0 is the laser wavelength in vacuum, E_{beam} is the electric field due to the electron beam, r_{41} is the only independent element of electro-optic tensor for the chosen crystal structure, and finally α is the angle between the electric field of the electron bunch and the $[-1, 1, 0]$ direction. This translates for our laser and a crystal of 100μm thickness and $\alpha = 0$ to values for Γ of respectively: 0.3 and 0.8 for ZnTe and for GaP, large enough to allow for single shot EO measurement.
Temporal resolution is also of major importance, thus we have included in our study the frequency dependence and we have calculated the propagation and the distortion of the THz pulse associated to the transient electric field for

several thicknesses of both ZnTe and GaP. The approach we have applied to the analysis of the FERMI case, is the one described in [6]. The crystal parameters used in these calculations are described in table 2.

Table 2: Crystal parameters.

Parameter	ZnTe	GaP
C	-0.07	-0.53
ν_0	5.3 THz	10.98 THz
Γ_0	0.09THz	0.02THz
d_E	$4 \cdot 10^{-12} m/V$	$1 \cdot 10^{-12} m/V$
ϵ_{el}	7.4	8.7
S_0	2.7	1.8
L_{char}	$30 \mu m$	42 μm

The underling idea is to divide the crystal in smaller slices where for each slice the laser beam has an different pulse width to calculate the total phase retardation as the sum of the individual slice phase retardation $\Gamma(t) = \sum_j \Gamma_j(\tau)$. Equation 4 shows how the calculation is performed.

$$\Gamma(t) = \frac{2\pi n_0^3 d}{\lambda_0} \sum_j \left[\int E^j_{slice}(t_{j,ls}) \frac{\exp \frac{-(t-\tau)^2}{2\sigma_j^2}}{\sqrt{2\pi}\sigma_j} dt \right] \quad (4)$$

At each slice:

$$t_{j,ls} = d_j / v_{gr} + \tau \quad (5)$$

and the laser pulse of σ_0 initial sigma, undergoes a broadening passing through the crystal, described by:

$$\sigma_j = \sigma_0 \sqrt{1 + \left(\frac{d_j}{L_{char}} \right)^2} \quad (6)$$

At the $j-th$ slice the electric field is defined in terms of the field at the $j-1$ slice using the Fourier Transforms (FT) and anti-transforms (IFT):

$$E^j_{slice}(t) = IFT \left\{ FT(E^{j-1}_{slice}(t_{j,ls})) A_{tr}(\nu) B_{tr}(\nu) r_{41}(\nu) \right\} \quad (7)$$

where A_{tr}, the amplitude transmission coefficient is :

$$A_{tr}(\nu) = \frac{1}{1 + n(\nu) + ik(\nu)} \quad (8)$$

and B_{ph} accounts for the phase propagation,

$$B_{ph}(\nu) = exp \left(\frac{i2\pi d_j n(\nu)\nu}{c} - \frac{2\pi d_j \kappa(\nu)\nu}{c} \right) \quad (9)$$

Finally the complex dielectric function $\epsilon(\nu)$ and $r_{41(\nu)}$ electro optic coefficient are modeled as damped oscillators:

$$\epsilon(\nu) = \epsilon_{el} + \frac{S_0 \nu_0^2}{\nu_0^2 - \nu^2 - i\Gamma_0 \nu} \quad (10)$$

$$r_{41}(\nu) = d_E \left(1 + \frac{C\nu_0^2}{\nu_0^2 - \nu^2 - i\Gamma_0 \nu} \right) \quad (11)$$

$$(12)$$

Where ϵ_{el} is the frequency independent electron component while S_0,ν_0,Γ_0 are respectively the oscillator strength, the TO crystal resonance frequency and the oscillator damping constant (and similarly for $r_{41}(\nu)$). The results for the calculation for the THz propagation as a function of the thickness show clear EO signal broadening and shape distortion occurs as the thickness of the crystal is increased. The distortion effect gets more and more severe as the the electron bunch gets shorter. Calculation for THz propagation in ZnTe are shown for crystal thickness from $50\mu m$ to 1mm in figures 2 and 3 respectively for the *Medium* and *Short* bunch cases.

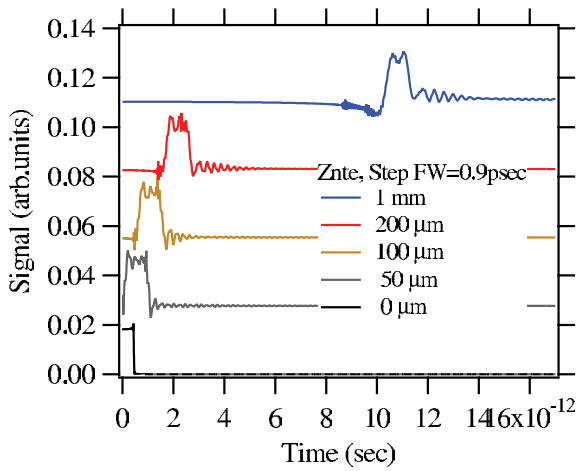

Figure 2: THz propagation through ZnTe crystal as a function of thickness for the *Medium Bunch*.

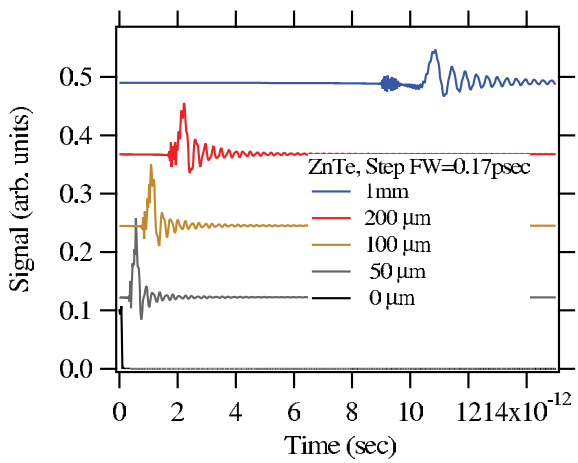

Figure 3: THz pulse propagation through ZnTe crystal as a function of thickness for the *Short Bunch*.

For the *Medium Bunch* negligible FWHM increase is found up to a Zn Te crystal thickness of 200 μm. Pulse shape distortion is present also for smaller thickness. For the *Short Bunch* the FWHM broadening is present even for $50\mu m$ and for 1mm thick ZnTe the width reaches 400fsec. Moreover strong pulse distortion is present for all thickness. Bet-

ter performances in terms of resolution and distortion are expected from GaP crystals due to its much higher crystal TO resonances which plays a crucial role in THz pulse propagation. We have performed for GaP the same kind of calculation done for ZnTe and the results are shown in figures 4 and 5 respectively for the *Medium* and *Short* bunch cases.

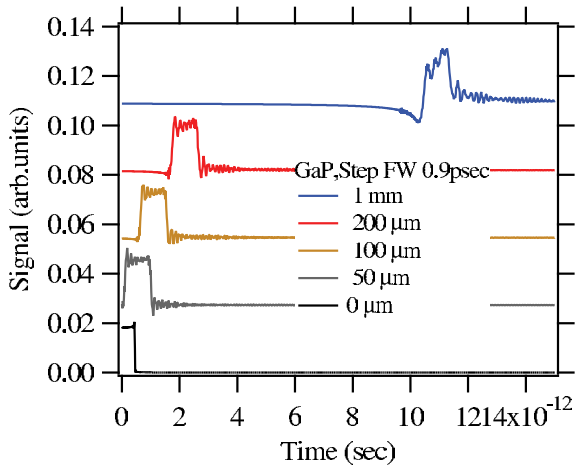

Figure 4: THz pulse propagation through GaP crystal as a function of thickness for the *Medium Bunch*.

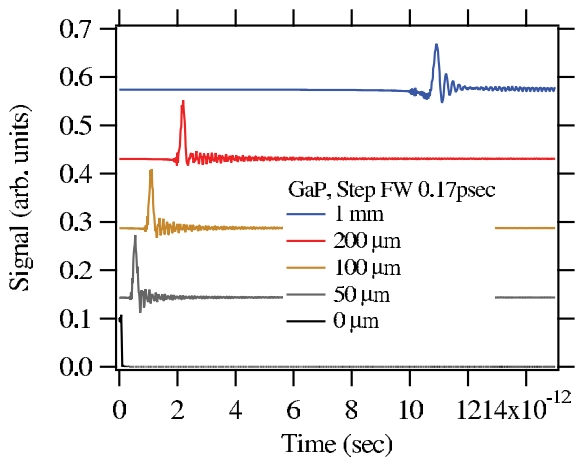

Figure 5: THz pulse propagation through GaP crystal as a function of thickness for the *Short Bunch*.

As expected GaP shows better performances in our case than ZnTe for both resolution and profile distortion in the both cases *Medium* and *Short bunch* but of course at the expense of a smaller electro optics coefficient. For the short bunch case FWHM is preserved within 10% for a GaP thinkness up to 200 μm but the THz profile is smoothed in the signal.

FEL ARRIVAL TIME

In a seeded FEL, the temporal jitter of FEL radiation depends not only on the arrival time of electron beam but and even more crucially from the temporal jitter of the seed laser. Timing of FEL radiation is of great interest for pump and probe experiments. Thee idea is to spill energy from the 800nm seed laser amplifier and use it for EOS measurements with the temporal decoding scheme. Temporal decoding has recently shown to be capable of 60 fsec resolution [4] better suited for the $ShortBunch$ mode of operation. For FERMI we could spill the radiation from the seed laser amplifier grating zero order beam and send it trough an evacuated transport line to the EOS. Considering the initial available energy and transport we estimate to have at the EOS station about 150μJ with a pulse length of 100fsec.

CONCLUSIONS

We have presented the design of the EOS stations for FERMI@Elettra. Major concepts and design choices have been introduced together with calculations of both expected EO signal strength and impact of THz e-beam electric field propagation in the EO crystals. Using the spatial decoding scheme coupled to a fiber laser source we aim at providing a robust and reliable system both to the machine operation and the user experiments. Benefits of expanding the EO stations to use the seed laser pulses for temporal decoding scheme are also discussed.

ACKNOWLEDGMENTS

The authors would like to thank P.Krejcik, D.Fritz for very useful discussion and suggestions on the spatial decoding scheme and S.P.Jamison for discussion and suggestions on the temporal decoding scheme.

REFERENCES

[1] FERMI CDR http://www.elettra.trieste.it/FERMI/

[2] A. Cavalieri et al. PRL 94 pg 114801 (2005)

[3] A. Azima et al. MOPCH011 Procs. EPAC 2006

[4] G. Berden et al. PRL 99, pg 164801 (2007)

[5] D.Fritz -LUSI team, private communication.

[6] S. Casalbuoni et al. TESLA Report 2005-01